


Article

Palladium Nanoparticles Supported on Graphene Oxide as Catalysts for the Synthesis of Diarylketones

Anna M. Trzeciak ^{1,*} , Przemysław Wojcik ¹, Radosław Lisiecki ², Yuriy Gerasymchuk ², Wiesław Strek ² and Janina Legendziewicz ¹

¹ Faculty of Chemistry, Wrocław University, 14 F. Joliot-Curie 14 St., 50-383 Wrocław, Poland; przemyslaw.wojcik@chem.uni.wroc.pl (P.W.); janina.legendziewicz@chem.uni.wroc.pl (J.L.)

² Institute of Low Temperature and Structure Research Polish Academy of Sciences, 2 Okólna St., 50-422 Wrocław, Poland; r.lisiecki@int.pan.wroc.pl (R.L.); j.gerasymchuk@int.pan.wroc.pl (Y.G.); w.strek@int.pan.wroc.pl (W.S.)

* Correspondence: anna.trzeciak@chem.uni.wroc.pl

Received: 5 March 2019; Accepted: 28 March 2019; Published: 1 April 2019



Abstract: Three palladium catalysts supported on graphene oxide (GO) and on its composite with TiO₂ (GO-TiO₂) were prepared and characterized. The presence of Pd NPs of different diameters (4–89 nm) and size distributions was evidenced by TEM measurements. GO-supported palladium efficiently catalysed the carbonylative coupling of iodobenzenes with aryl boronic acids forming relevant diarylketones at 1 atm CO. The highest activity and recyclability were obtained for Pd/GO-TiO₂. The emission behaviour of Pd/GO and Pd/GO-TiO₂ catalysts indicated structural changes occurring during the catalytic reaction.

Keywords: palladium; graphene oxide; carbonylative coupling

1. Introduction

Carbon-based materials, such as graphene oxide (GO), reduced graphene oxide, multi-walled carbon nanotubes, and single-walled carbon nanotubes have already found many applications due to their physical and mechanical properties [1–4]. In particular, the electronic and optic properties of GO can be controlled by the ratio of the sp²–to–sp³ hybridized carbons [5–8]. This is important for applications of GO in material chemistry and technology as transistors or sensors. Graphene oxide (GO) is also a promising material for the development of new immobilized metal catalysts, in particular containing palladium as an active phase [9–11]. The immobilization of the catalyst enables its efficient separation from organic products and use in subsequent catalytic runs. For these functions, the support should perfectly stabilize catalytically active palladium forms and prevent their leaching to the solution. Porous GO materials with a layered structure containing different functional groups able to form stable bonds with metals meet these expectations perfectly. In addition, a high surface-to-weight ratio, low mass density, and accessibility of differently modified centres make it possible to select GO for catalytic applications. The successful use of Pd/GO in the Suzuki–Miyaura reaction has been reported [12–25]. Not only high conversion but also good catalyst recyclability have been achieved. Only one example of the use of Pd/GO in the carbonylative Suzuki–Miyaura coupling leading to aryl ketones has so far been reported [26].

Because the interatomic distance of Pd (0.225 nm) is close to the honeycomb spacing in graphene (0.240 nm), bonding between Pd and GO is possible [27]. The introduction of Pd to GO resulted in a decrease in the number of oxygen functional defects, while the number of sp² carbon atoms and delocalized π -electrons increased. The change of the GO structure led to the modification of its optical properties including photoluminescence. Further changes of the optical properties could be expected

as a result of the structural changes of the Pd/GO composite under catalytic conditions, but this aspect has not been studied yet.

Our studies aimed at the synthesis of Pd/GO and Pd/GO-TiO₂ catalysts and testing their activity in the carbonylative Suzuki–Miyaura coupling. By the introduction of TiO₂ to the GO support, we expected to increase the stability and recyclability of the palladium catalyst. Moreover, the presence of TiO₂ increased the photocatalytic activity of GO [28,29]. The structural characteristics of the GO-immobilized palladium catalysts were obtained using different methods, including measurements of emission spectra. It was expected that the emission behaviour of the studied samples would be helpful in understanding the structural changes of the catalyst during the catalytic process.

2. Results and Discussion

Two catalysts supported on GO, Pd/GO-A and Pd/GO-B, were obtained by different procedures. Pd/GO-A was prepared from PdCl₂ as the palladium source, in an acetonitrile solution at RT without any additional reducing agent. The TEM analysis evidenced the presence of 34–89 nm Pd NPs, partially agglomerated (Figure 1). Characteristic lines of the crystalline Pd NPs and GO were observed in the XRD picture (Figure 2). The second palladium catalyst, Pd/GO-B, was obtained according to the literature method [24], using Pd(OAc)₂ as the substrate and a sonication step as part of the synthetic procedure. The obtained composite, Pd/GO-B, contained Pd NPs of *ca.* 8–9 nm in diameter with a relatively narrow size distribution (Figure 3). The palladium content in Pd/GO-B was higher than in Pd/GO-A according to the ICP analysis. On the other hand, an EDX analysis showed lower Pd content values on the surface of Pd/GO-B than on the surface of Pd/GO-A.

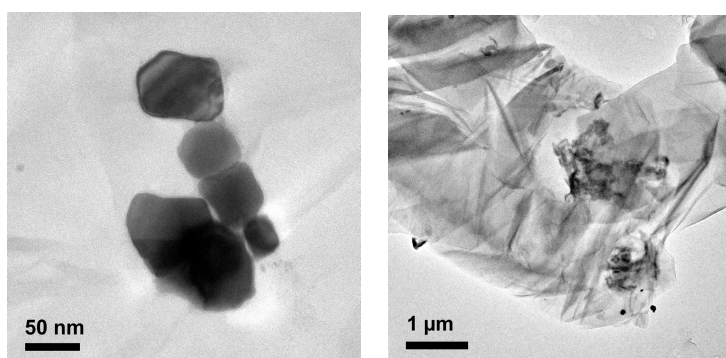


Figure 1. TEM pictures of Pd/GO-A.

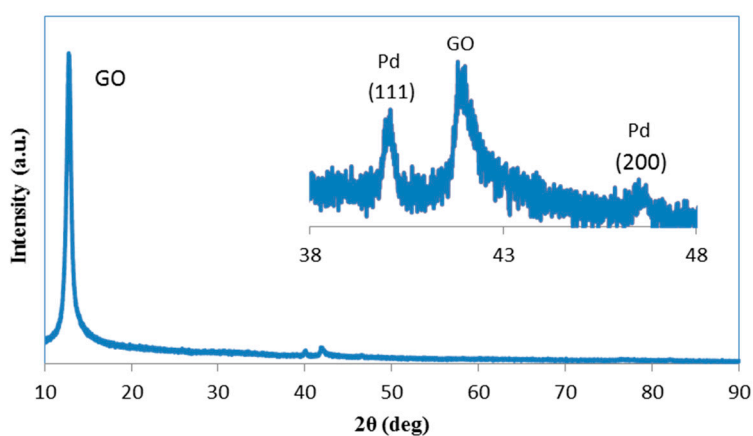


Figure 2. XRD of Pd/GO-A.

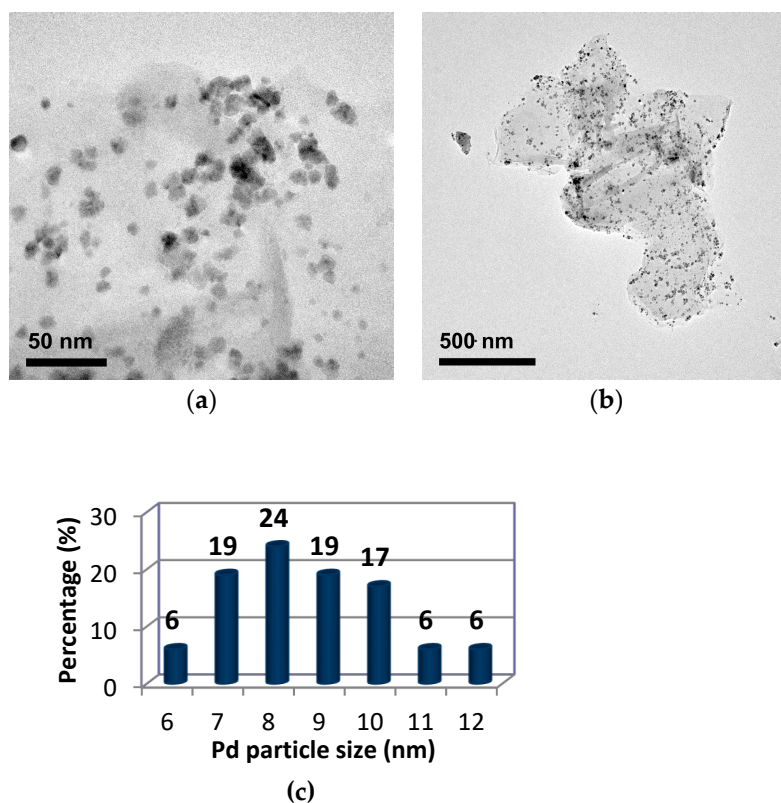


Figure 3. TEM pictures (a,b) and Pd NPs size distribution (c) for Pd/GO-B.

The synthesis of Pd/GO-TiO₂ was performed according to the method used for Pd/GO-A. The presence of TiO₂ in the support resulted in formation of small Pd NPs, uniformly distributed on the surface, as shown by the TEM pictures. However, the SEM/EDX analysis indicated low palladium amounts on the surface (0.01–0.06 atom%). Moreover, the XRD measurement presented only lines originating from GO-TiO₂. The palladium lines were not visible, probably because of the small diameter of Pd NPs. It can be assumed that palladium in Pd/GO-TiO₂ was localized mostly inside the support material, but not on its surface.

2.1. Catalytic Activity of Pd/GO

The activity of Pd/GO and Pd/GO-TiO₂ catalysts was investigated in the carbonylative Suzuki–Miyaura cross-coupling of 4-iodoanisole with phenylboronic acid at 1 atm of CO (Figure 4, Table 1).

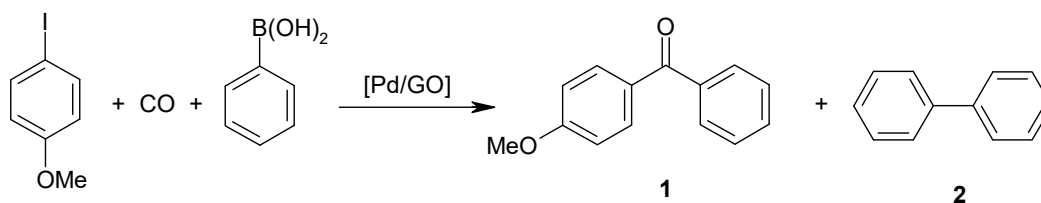


Figure 4. The carbonylative Suzuki–Miyaura reaction.

Table 1. The carbonylative Suzuki–Miyaura reaction with GO-supported palladium ^a.

Entry	Catalyst	Conversion (%)	Yield 1 (%)	Yield 2 (%)	Selectivity to 1 (%)
1	Pd/GO-A	78	70	7	91
2	Pd/GO-B	82	74	7	90
3	Pd/GO-TiO ₂	95	89	6	94
4	Pd/C (10%)	88	82	6	93

Reaction conditions: 4-iodoanisole (1 mmol); PhB(OH)₂ (1.2 mmol); 0.2 mol% [Pd], 3 mmol K₂CO₃, 1 atm CO, 5 mL anisole, 4 h, 100 °C. ^a Determined by GC using dodecane as the internal standard.

Under the applied conditions, all the catalysts studied showed a high activity and good selectivity to the desired ketone. The Pd/GO-A with the lowest palladium content (0.26 wt%) and agglomerated Pd NPs presented the lowest catalytic activity, while the Pd/GO-B containing smaller and dispersed Pd NPs gave a slightly higher conversion. Among these three catalysts, Pd/GO-TiO₂ turns out to present the highest catalytic activity with a conversion 95% and a selectivity to ketone of 94%. These results were also better than those obtained using a commercial Pd/C catalyst (88% conversion).

2.2. Optimization of the Reaction Conditions for Pd/GO-TiO₂

The influence of the reaction parameters, such the amount of the base, temperature and reaction time, was studied for the Pd/GO-TiO₂ catalyst (Table 2).

Table 2. Optimization of the carbonylative Suzuki–Miyaura reaction using Pd/GO-TiO₂ ^a.

Entry	Catalyst Loading (mol%)	K ₂ CO ₃ (mmol)	Solvent	Temp. (°C)	Time (h)	Conversion (%)	Yield 1 (%)	Yield 2 (%)
1	0.23	3	Anisole	100	5	96	91	5
2	0.2	3	Anisole	100	4	95	89	6
3	0.2	2	Anisole	100	4	92	85	7
4	0.2	1	Anisole	100	4	77	72	5
5	0.2	3	Anisole	100	3	81	79	2
6	0.2	3	Dioxane	100	3	60	55	5
7	0.2	3	Anisole	80	3	51	51	0
8	0.2	3	Water	80	3	26	5	21

Reaction conditions: 4-iodoanisole (1 mmol); PhB(OH)₂ (1.2 mmol); 1 atm CO, 5 mL solvent, 4 h, 100 °C.

^a Determined by GC using dodecane as the internal standard.

A reaction time of 4 h was sufficient for the maximum 95% conversion, while 81% was achieved after 3 h. Lowering the amount of K₂CO₃ from 3 to 1 mmol resulted in a conversion decrease to 77% due to a less efficient transmetallation process. Changing the solvent from anisole to dioxane caused a decrease in conversion, while water promoted the formation of the Suzuki–Miyaura product.

The influence of the daylight was also investigated considering possible photoactivation with TiO₂. However the results obtained with or without exposure to light were practically the same.

2.3. Substrate Screening in the Carbonylative Suzuki–Miyaura Coupling

The optimized reaction conditions were next used in investigations of reactions with different aryl iodides and aryl boronic acids catalysed by the Pd/GO-TiO₂ catalyst (Figure 5, Table 3).

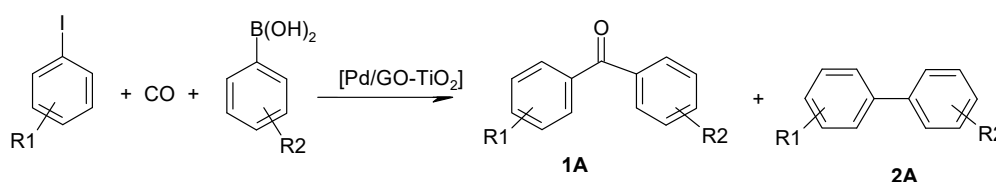
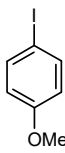
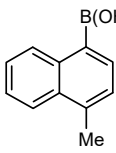
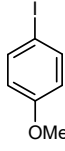
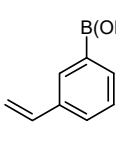
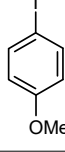
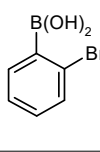
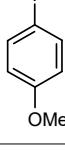
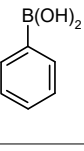
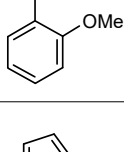
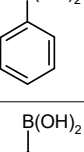
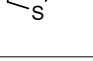
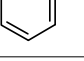
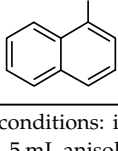
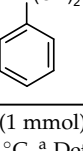
**Figure 5.** The carbonylative Suzuki–Miyaura reaction.

Table 3. Substrate screening using Pd/GO-TiO₂ ^a.

Entry	Iodoarene	Arylboronic Acid	Conversion (%)	Yield 1A (%)	Yield 2A (%)	Selectivity to 1A (%)
1			95	66 (57 ^b)	27	72
2			56	52	4	93
3			73	55 (42 ^b)	18	75
4			95	89 (80 ^b)	6	94
5			87	62 (50 ^b)	25	71
6			97	85 (77 ^b)	12	88
7			97	69 (58 ^b)	28	71

Reaction conditions: iodoarene (1 mmol), arylboronic acid (1.2 mmol), Pd/GO-TiO₂ 0.2 mol%, 3 mmol K₂CO₃, 1 atm CO, 5 mL anisole, 4 h, 100 °C. ^a Determined by GC using dodecane as the internal standard. ^b Yield of the isolated product.

The Pd/GO-TiO₂ catalyst also provided very good results in both conversion and selectivities by using different aryl iodides and aryl boronic acids under the optimized reaction conditions. The best conversions were achieved using 4-methyl-1-naphthaleneboronic acid, phenylboronic acid, 2-iodothiophene, and 1-iodonaphthalene (entries 1, 4, 6, 7). The highest selectivity to ketone was obtained by using 3-vinyl-phenylboronic acid and phenylboronic acid (entries 2, 4).

All in all, conversions up to 97% as well as selectivity to ketone up to 94% could be achieved using a Pd/GO-TiO₂ catalyst.

2.4. Recycling of Pd/GO-B and Pd/GO-TiO₂ Catalysts

Attempts at catalyst recycling were performed for Pd/GO-B and Pd/GO-TiO₂ (Table 4). The first carbonylative Suzuki–Miyaura reaction was carried out under the given reaction conditions. Next, the organic products were extracted with hexane, and a new portion of the reactants was added to the catalyst remaining in the anisole solution. The activity of the Pd/GO-B catalyst decreased rather fast in subsequent runs, and conversion dropped from 87% in the first reaction to 48% in the third one.

In contrast, Pd/GO-TiO₂ was more stable, and a conversion decrease from 97% to 80% was noted after four runs. During recycling, some decrease of the selectivity to ketone was observed as a result of 2-methylbiphenyl, the product formed by the normal Suzuki–Miyaura coupling.

Table 4. Recycling of Pd/GO-TiO₂ in the carbonylative Suzuki–Miyaura cross-coupling reaction ^a.

Entry	Recycling Run	Conversion (%)	Yield 1 (%)	Yield 2 (%)	Selectivity to 1 (%)
1	0	97	94	3	97
2	1	98	82	16	84
3	2	84	66	18	78
4	3	80	63	17	79

Reaction conditions: 4-iodoanisole (1 mmol); PhB(OH)₂ (1.2 mmol); 0.17 mol% [Pd], 3 mmol K₂CO₃, 1 atm CO, 5 mL anisole, 4 h, 100 °C. ^a Determined by GC using dodecane as the internal standard.

The observed decrease of catalytic activity during recycling can be explained, at least partially, by the loss of some palladium during extraction of products. It should also be stressed that the recycling experiments were performed using only 0.17% of Pd/GO-TiO₂.

In order to determine whether the Pd nanoparticles are responsible for the catalytic activity, the mercury test was performed [30]. According to the literature, the addition of Hg(0) to the reaction mixture should result in the formation of inactive Pd/Hg amalgam and retarding of the catalytic process. When 500-fold excess of Hg(0) was added to the catalytic system together with substrates, no conversion of iodobenzene was noted. Therefore, it is reasonable to conclude that in this reaction palladium nanoparticles are involved in the catalytic process taking place on their surface. On the other hand, SEM/EDX analyses shown small decrease of Pd content on the surface of Pd/GO-TiO₂ from 0.2–0.25 atom% before catalytic reaction to 0.2–0.22 atom% after the reaction, indicating on possible palladium leaching. In conclusion, we propose contribution of both, palladium nanoparticles and underligated palladium species, in the catalytic process.

2.5. Luminescent Studies of Pd/GO Catalysts

After the characterization of the catalytic properties of palladium supported on GO materials, spectroscopic studies were undertaken to get deeper knowledge about structural changes occurring during the reaction (see Figure 6). We used excitation lines (λ_{ex} = 300, 445, 488, 800 nm) similar to those in the excitation of graphene ceramics. In the case of GO emission, the observed shapes of emission bands were similar regardless of the excitation lines used. However, their intensities were different. For example, the intensity of the emission for λ_{ex} = 488 nm was significantly lower for GO-TiO₂ than for GO, due to the recombination decrease in the electron-hole process after C-Ti bond formation.

The addition of Pd to GO and GO-TiO₂ materials caused a remarkable increase in emission intensity for λ_{ex} = 800 nm and 445 nm. The same effect was also noted using λ_{ex} = 488 nm for GO-TiO₂, while grafting of Pd on GO did not change this emission intensity. The enhanced blue emission after the introduction of Pd indicated the reduction of GO and increase in the number of π -electrons [27].

Further changes of emission spectra were observed in samples recovered after the catalytic process. A comparison of emission spectra of Pd/GO-TiO₂ before and after the catalytic reaction (Pd/GO-TiO₂-R) showed a significant decrease in emission intensity at λ_{ex} = 445 and 488 nm. For 800 nm, however, the line became broader, and its intensity decreased only slightly. Significant changes were detected in the shapes and intensities of the lines in the spectra of Pd/GO and Pd/GO-R. In all three experiments, the emission lines measured for the post-reaction samples (Pd/GO-R) presented the highest intensity. It is worth noting that the reactants used in the catalytic process did not emit in the studied spectra range. Therefore, the observed changes can be interpreted in relation to the structural changes of Pd/GO catalysts.

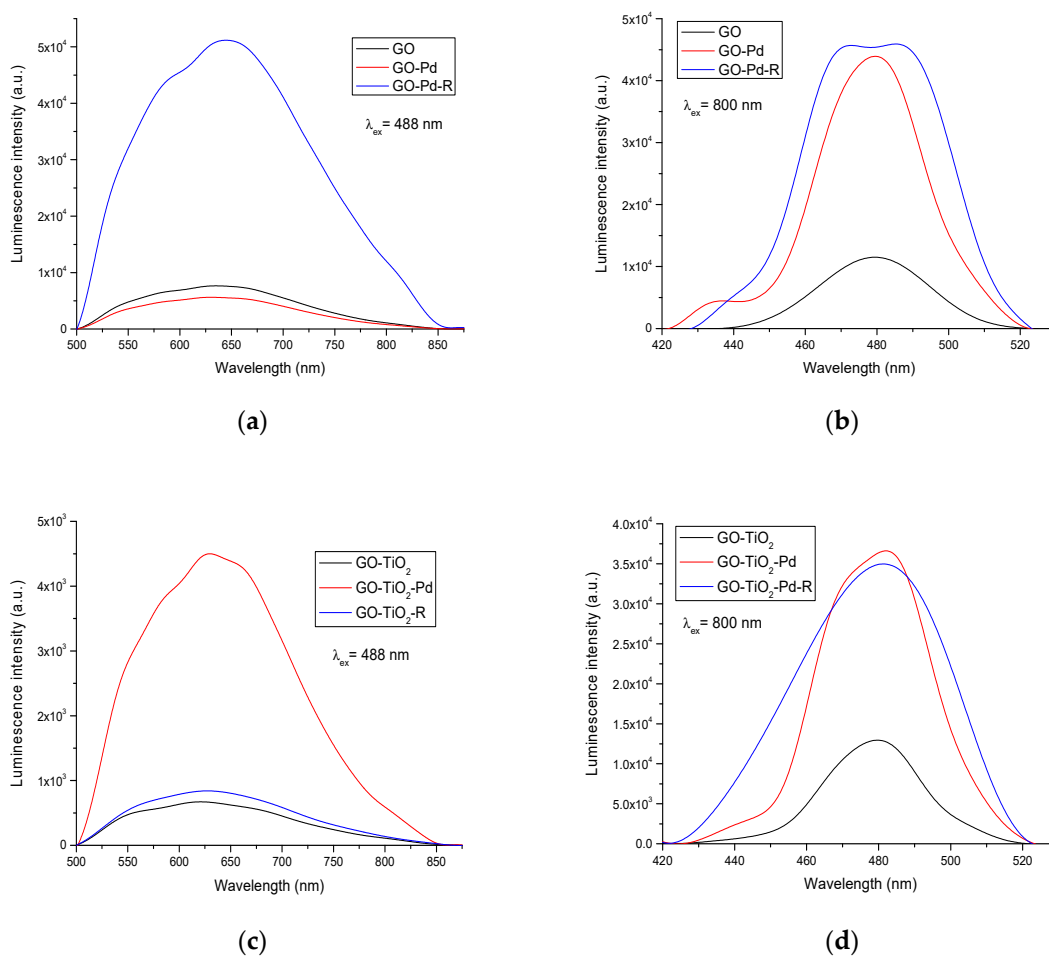


Figure 6. Emission spectra of Pd/GO (a,b) and Pd/GO-TiO₂ (c,d) at different excitation lines.

The analysis of emission spectra indicated different behaviours of Pd/GO-TiO₂ and Pd/GO under the catalytic conditions (see Supplementary Materials). The observed decrease in line intensities observed for Pd/GO-TiO₂ can be explained by a decrease in the number of sp² clusters in the GO composite. Although the mechanism of the emission process is not fully explained, the observed effects suggested the participation of the GO-TiO₂ support in the catalytic reaction. Such synergistic interaction of palladium and the support can increase the catalytic activity and stability of the Pd/GO-TiO₂ catalyst.

3. Experimental

3.1. Synthesis of Pd/GO-A

Graphene oxide (GO, 0.2 g) [31] was placed in a 50 mL flask, and 10 mL of dry acetonitrile was added. In a second 50 mL flask, the PdCl₂(MeCN)₂ complex (0.1 g) was solved in 20 mL of dry acetonitrile. The solution of the palladium complex was slowly added to the stirred solution of GO under a nitrogen atmosphere. The reaction mixture was stirred for 1 day at RT. Next, the solution was filtered, and the obtained solid was washed with diethyl ether (20 mL) and acetonitrile (15 mL) and dried. Yield: 166 mg. The palladium content (according to ICP analysis) was 0.26 weight %. The Pd/GO-A was also analysed by TEM, SEM, and XRD (Figures 1, 2 and 7).

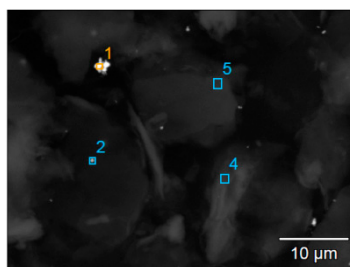


Figure 7. SEM pictures of Pd/GO-A. The content of Pd ranged from 0.28 to 10.20 atom% and the Cl content was 0.18–0.36 atom%.

3.2. Synthesis of Pd/GO-B

Graphene oxide (GO, 0.2 g) [31] and $\text{Pd}(\text{OAc})_2$ (0.1 g) were dissolved in 40 mL of dry toluene under a nitrogen atmosphere. The reaction mixture was sonicated for 50 min, heated under reflux for 1 h, and then stirred for 1 day at RT. Next, the solution was filtered, and the obtained solid was washed with diethyl ether (15 mL), ethanol (15 mL), and acetone (10 mL) and dried. Yield: 152 mg. The palladium content (according to ICP analysis) was 4.95 weight%. The Pd/GO-B was analysed by TEM, SEM, and XRD (Figures 3, 8 and 9).

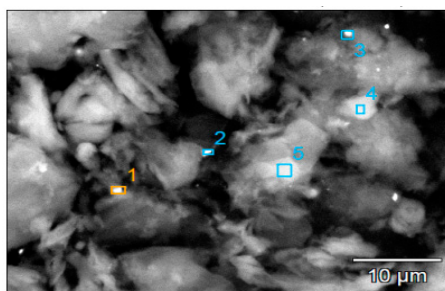


Figure 8. SEM picture of Pd/GO-B. The content of Pd ranged from 0.23 to 2.99 atom% and the Cl content was 0.21–0.28 atom%.

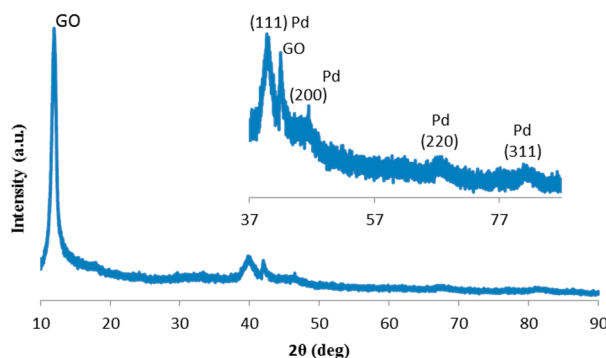


Figure 9. XRD of Pd/GO-B.

3.3. Synthesis of Pd/GO-TiO₂

Titanium-dioxide-modified graphene oxide (GO-TiO₂, 0.346 g) [28] was placed in a 50 mL flask, and 10 mL of dry acetonitrile was added. In a second 50 mL flask, the $\text{PdCl}_2(\text{MeCN})_2$ complex (0.173 g) was dissolved in 20 mL of dry acetonitrile. The solution of the palladium complex was slowly added to the stirred solution of GO-TiO₂ under nitrogen atmosphere. The reaction mixture was stirred for 1 day at RT. Next, the solution was filtered, and the obtained solid was washed with diethyl ether (20 mL) and acetonitrile (15 mL) and dried. Yield: 322 mg. The palladium content (according to ICP analysis) was 1.21 weight%. The Pd/GO-TiO₂ was analysed by TEM, SEMs and XRD (Figures 10 and 11).

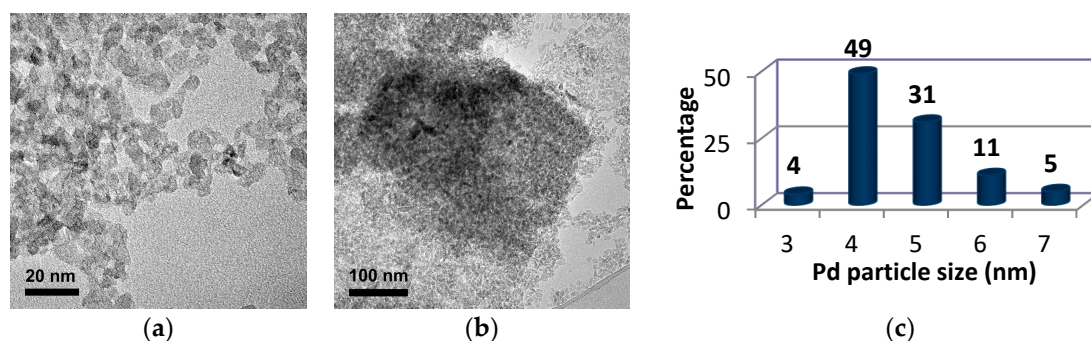


Figure 10. TEM pictures (a,b) and Pd NPs size distribution (c) for Pd/GO-TiO₂.

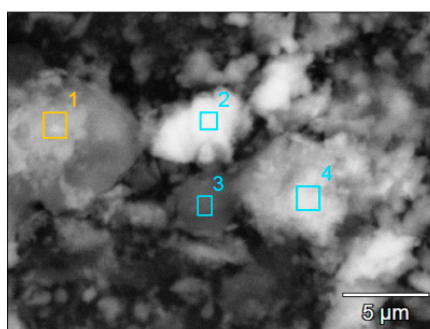


Figure 11. SEM picture of Pd/GO-TiO₂. The content of Pd ranged from 0.01 to 0.06 atom% and The Cl content was 0.52–1.87 atom%.

3.4. Electron Absorption and Emission Spectra

Room temperature electron absorption spectra were measured in the 200–1500 nm spectral range using a Cary-Varian 5E UV-VIS-near-IR spectrophotometer (Palo Alto, CA, USA). In the case of a weak signal of the spectrum, the spectrophotometer was switched to measurements in the reflectance mode.

Emission spectra were achieved using an excitation source consisting of a femtosecond laser (Coherent Model “Libra”) coupled to an optical parametric amplifier (Light Conversion Model “OPerA”). The system delivers 100 fs pulses at a repetition rate regulated up to 1 kHz at a wavelength tuned between 230–2800 nm. The excitation light was focused on samples using lens with a focal length of 15 cm. The sample luminescence was observed in the direction perpendicular to the excitation beam. Appropriate long-pass filters were used to eliminate unwanted radiation. Emission spectra and luminescence decay curves were recorded with a grating spectrograph (Princeton Instr. Model Acton 2500i, Princeton, NJ, USA) coupled to a streak camera (Hamamatsu Model C5680, Tokyo, Japan), operating in the 200–1100 nm spectral region with a temporal resolution of 20 ps. A number of excitation laser sources were used, from the visible (VIS) up to the near-infrared (NIR) regime:

GC-FID and GC/MS measurements of organic products were performed using an HP5890 (Hewlett Packard, Palo Alto, CA, USA) instrument with a 5971A mass detector. Organic products were separated by flash chromatography (CombiFlash Rf 200, Changzhou, China) on silica gel.

ICP measurements of the palladium content were performed using an ARL 3410 model spectrometer. TEM measurements were carried out using a FEI Tecnai G² 20 X-TWIN electron microscope operating at 200 kV (Waltham, MA, USA).

4. Conclusions

The nanosize palladium catalysts, supported on GO and GO-TiO₂ were prepared from PdCl₂(MeCN)₂ and Pd(OAc)₂. An effect of the palladium precursor and the synthetic method on the structure of the catalyst was confirmed by physicochemical methods. The introduction of Pd to the GO matrix resulted in an increase in photoemission due to an increase in the number of sp²

centres. The GO-supported palladium exhibited high activity and selectivity in the carbonylative Suzuki–Miyaura coupling producing the relevant diarylketones at 1 atm CO and a low amount of the catalyst (0.2 mol%). The best productivity, over 95% of the ketone, was noted for Pd/GO-TiO₂, which was also successfully recycled in four subsequent runs. The emission spectra of the Pd/GO-TiO₂ catalyst recovered after the catalytic process showed a decrease in the band intensity. This can be explained by the structural change and a recombination decrease in the electron-hole process. A better understanding of the emission process mechanism in Pd/GO composites requires further studies. However, our results showed that emission spectra can provide useful information about these catalytic systems.

Supplementary Materials: The following are available online at <http://www.mdpi.com/2073-4344/9/4/319/s1>, Figure S1: Emission spectra of Pd/GO and Pd/GO-TiO₂ at λ_{ex} = 445 nm.

Author Contributions: Conceptualization, A.M.T., W.S. and J.L.; Methodology, A.M.T., J.L.; Investigation, P.W., Y.G. and R.L.; Data curation, P.W. and R.L.; Writing—original draft preparation, A.M.T. and J.L.; Writing—review and editing, A.M.T. and J.L.; Supervision, A.M.T.; Funding acquisition, A.M.T.

Acknowledgments: Financial support of National Science Foundation (NCN) with grant 2017/25/B/ST5/00394 is gratefully acknowledged (AT). Authors are grateful to Marek Hojniak (Faculty of Chemistry, University of Wrocław) for GC and GC-MS analysis, to Wojciech Gil (Faculty of Chemistry, University of Wrocław) for performing SEM and TEM measurements and to Sebastian Demmler (Leipzig University) for performance of catalytic studies.

Conflicts of Interest: The authors declare no conflict of interest.

References

1. Iijima, S. Helical microtubules of graphitic carbon. *Nature* **1991**, *354*, 56–58. [CrossRef]
2. Baughman, R.H.; Zakhidov, A.A.; de Heer, W.A. Carbon Nanotubes—The Route toward Applications. *Science* **2002**, *297*, 787–792. [CrossRef]
3. Castro, M.; Lu, J.; Bruzard, S.; Kumar, B.; Feller, J.F. Carbon nanotubes/poly (ϵ -caprolactone) composite vapour sensors. *Carbon* **2009**, *47*, 1930–1942. [CrossRef]
4. Loh, K.P.; Bao, Q.; Eda, G.; Chhowalla, M. Graphene oxide as a chemically tunable platform for optical applications. *Nat. Chem.* **2010**, *2*, 1015–1024. [CrossRef]
5. Liu, Z.; Wang, Y.; Zhang, X.; Xu, Y.; Chen, Y.; Tian, J. Nonlinear optical properties of graphene oxide in nanosecond and picosecond regimes. *Appl. Phys. Lett.* **2009**, *94*, 021902. [CrossRef]
6. Eda, G.; Mattevi, C.; Yamaguchi, H.; Kim, H.K.; Chhowalla, M. Insulator to Semimetal Transition in Graphene Oxide. Materials Science and Engineering, Rutgers University, Piscataway, New Jersey 08854. *J. Phys. Chem. C* **2009**, *113*, 15768–15771. [CrossRef]
7. Omidvar, A.; Rashidian Vaziri, M.R.; Jaleh, B. Enhancing the nonlinear optical properties of graphene oxide by repairing with palladium nanoparticles. *Phys. E Low Diment. Syst. Nanostruct.* **2018**, *103*, 239–245. [CrossRef]
8. Narayanam, P.K.; Sankaran, K. Optical behaviour of functional groups of graphene oxide. *Mater. Res. Express* **2016**, *3*, 105604. [CrossRef]
9. Rumi, L.; Scheuermann, G.M.; Mülhaupt, R.; Bannwarth, W. Palladium Nanoparticles on Graphite Oxide as Catalyst for Suzuki–Miyaura, Mizoroki–Heck, and Sonogashira Reactions. *Helv. Chim. Acta* **2011**, *94*, 966–976. [CrossRef]
10. Veisi, H.; Mirzaee, N. Ligand-free Mizoroki–Heck reaction using reusable modified graphene oxide-supported Pd(0) nanoparticles. *Appl. Organomet. Chem.* **2018**, *32*, e4067. [CrossRef]
11. Cheng, J.; Zhang, G.; Du, J.; Tang, L.; Xu, J.; Li, J. New role of graphene oxide as active hydrogen donor in the recyclable palladium nanoparticles catalyzed Ullmann reaction in environmental friendly ionic liquid/supercritical carbon dioxide system. *J. Mater. Chem.* **2011**, *21*, 3485–3494. [CrossRef]
12. Hemant Joshi, H.; Sharma, K.N.; Sharma, A.K.; Singh, A.K. Palladium–phosphorus/sulfur nanoparticles (NPs) decorated on graphene oxide: Synthesis using the same precursor for NPs and catalytic applications in Suzuki–Miyaura coupling. *Nanoscale* **2014**, *6*, 4588–4597. [CrossRef] [PubMed]

13. Gao, S.; Shang, N.; Feng, C.; Wang, C.; Wang, Z. Graphene oxide–palladium modified Ag–AgBr: A visible-light-responsive photocatalyst for the Suzuki coupling reaction. *RSC Adv.* **2014**, *4*, 39242–39247. [[CrossRef](#)]
14. Singh, V.V.; Kumar, U.; Tripathi, S.N.; Singh, A.K. Shape dependent catalytic activity of nanoflowers and nanospheres of Pd₄S generated via one pot synthesis and grafted on graphene oxide for Suzuki coupling. *Dalton Trans.* **2014**, *43*, 12555–12563. [[CrossRef](#)]
15. Wang, X.; Chen, W.; Yan, L. Three-dimensional reduced graphene oxide architecture embedded palladium nanoparticles as highly active catalyst for the Suzuki–Miyaura coupling reaction. *Mater. Chem. Phys.* **2014**, *148*, 103–109. [[CrossRef](#)]
16. Hoseini, S.J.; Khozestan, H.G.; Fath, R.H. Covalent attachment of 3-(aminomethyl)pyridine to graphene oxide: A new stabilizer for the synthesis of a palladium thin film at the oil–water interface as an effective catalyst for the Suzuki–Miyaura reaction. *RSC Adv.* **2015**, *5*, 47701–47708. [[CrossRef](#)]
17. Scheuermann, G.M.; Rumi, L.; Steurer, P.; Bannwarth, W.; Rolf Mülhaupt, R. Palladium Nanoparticles on Graphite Oxide and Its Functionalized Graphene Derivatives as Highly Active Catalysts for the Suzuki–Miyaura Coupling Reaction. *J. Am. Chem. Soc.* **2009**, *131*, 8262–8270. [[CrossRef](#)] [[PubMed](#)]
18. Siamaki, A.R.; Khder, A.E.R.S.; Abdelsayed, V.; El-Shall, M.S.; Gupton, B.F. Microwave-assisted synthesis of palladium nanoparticles supported on graphene: A highly active and recyclable catalyst for carbon–carbon cross-coupling reactions. *J. Catal.* **2011**, *279*, 1–11. [[CrossRef](#)]
19. Moussa, S.; Siamaki, A.R.; Gupton, B.F.; El-Shall, M.S. Pd-Partially Reduced Graphene Oxide Catalysts (Pd/PRGO): Laser Synthesis of Pd Nanoparticles Supported on PRGO Nanosheets for Carbon–Carbon Cross Coupling Reactions. *ACS Catal.* **2012**, *2*, 145–154. [[CrossRef](#)]
20. Nishina, Y.; Miyata, J.; Kawai, R.; Gotoh, K. Recyclable Pd–graphene catalyst: Mechanistic insights into heterogeneous and homogeneous catalysis. *RSC Adv.* **2012**, *2*, 9380–9382. [[CrossRef](#)]
21. Sayedi, N.; Saidi, K.; Sheibani, H. Green Synthesis of Pd nanoparticles supported on magnetic graphene oxide by *Origanum vulgare* leaf plant extract: Catalytic activity in the reduction of organic dyes and Suzuki–Miyaura cross-coupling reaction. *Catal. Lett.* **2018**, *148*, 277–288. [[CrossRef](#)]
22. Surjakanta Rana, S.; Maddila, S.; Yalagala, K.; Jonnalagadda, S.B. Organo functionalized graphene with Pd nanoparticles and its excellent catalytic activity for Suzuki coupling reaction. *Appl. Catal. A Gen.* **2015**, *505*, 539–547. [[CrossRef](#)]
23. Shang, N.; Gao, S.; Feng, C.; Zhang, H.; Wang, C.; Wang, Z.; Gao, S.; Feng, C.; Zhang, H.; Wang, C.; Wang, Z. Graphene oxide supported N-heterocyclic carbene–palladium as a novel catalyst for the Suzuki–Miyaura reaction. *RSC Adv.* **2013**, *3*, 21863–21868. [[CrossRef](#)]
24. Santra, S.; Hota, P.K.; Bhattacharyya, R.; Bera, P.; Ghosh, P.; Mandal, S.K. Palladium Nanoparticles on Graphite Oxide: A Recyclable Catalyst for the Synthesis of Biaryl Cores. *ACS Catal.* **2013**, *3*, 2776–2789. [[CrossRef](#)]
25. Gómez-Martínez, M.; Baeza, A.; Alonso, D.A. Graphene Oxide-Supported Oxime Palladacycles as Efficient Catalysts for the Suzuki–Miyaura Cross-Coupling Reaction of Aryl Bromides at Room Temperature under Aqueous Conditions. *Catalysts* **2017**, *7*, 94. [[CrossRef](#)]
26. Biying, A.O.; Vangala, V.R.; Chen, C.S.; Stubbs, L.P.; Hosmane, N.S.; Yinghuai, Z. Cross-coupling reaction between arylboronic acids and carboranyl iodides catalyzed by graphene oxide (GO)-supported Pd(0) recyclable nanoparticles for the synthesis of carboranylaryl ketones. *Dalton Trans.* **2014**, *43*, 5014–5020. [[CrossRef](#)]
27. Rani, J.R.; Oh, J.; Park, J.; Lim, J.; Park, B.; Kim, K.; Kim, S.-J.; Jun, S.C. Controlling the luminescence emission from palladium grafted graphene oxide thin films via reduction. *Nanoscale* **2013**, *5*, 5620–5627. [[CrossRef](#)]
28. Min, Y.L.; Zhang, K.; Zhao, W.; Zheng, F.C.; Zhang, Y.G. Enhanced chemical interaction between TiO₂ and graphene oxide for photocatalytic decolorization of methylene blue. *Chem. Eng. J.* **2012**, *193–194*, 203–210. [[CrossRef](#)]
29. Huang, Q.; Tian, S.; Zeng, D.; Wang, X.; Song, W.; Li, Y.; Xiao, W.; Xie, C. Enhanced Photocatalytic Activity of Chemically Bonded TiO₂/Graphene Composites Based on the Effective Interfacial Charge Transfer through the C–Ti Bond. *ACS Catal.* **2013**, *3*, 1477–1485. [[CrossRef](#)]

30. Phan, N.T.S.; van Der Sluys, M.; Jones, C.W. On the Nature of the Active Species in Palladium Catalyzed Mizoroki–Heck and Suzuki–Miyaura Couplings—Homogeneous or Heterogeneous Catalysis, A Critical Review. *Adv. Synth. Catal.* **2006**, *348*, 609–680. [[CrossRef](#)]
31. Szabó, T.; Tombácz, E.; Illés, E.; Dékány, I. Enhanced acidity and pH-dependent surface charge characterization of successively oxidized graphite oxides. *Carbon* **2006**, *44*, 537–545. [[CrossRef](#)]



© 2019 by the authors. Licensee MDPI, Basel, Switzerland. This article is an open access article distributed under the terms and conditions of the Creative Commons Attribution (CC BY) license (<http://creativecommons.org/licenses/by/4.0/>).